



## A green and efficient route for P – S – C bond construction using copper ferrite nanoparticles as catalyst: a TD-DFT study

Firouz Matloubi Moghaddam , Maryam Daneshfar & Reza Azaryan

To cite this article: Firouz Matloubi Moghaddam , Maryam Daneshfar & Reza Azaryan (2020): A green and efficient route for P – S – C bond construction using copper ferrite nanoparticles as catalyst: a TD-DFT study, Phosphorus, Sulfur, and Silicon and the Related Elements, DOI: [10.1080/10426507.2020.1833331](https://doi.org/10.1080/10426507.2020.1833331)

To link to this article: <https://doi.org/10.1080/10426507.2020.1833331>



View supplementary material [↗](#)



Published online: 26 Oct 2020.



Submit your article to this journal [↗](#)



View related articles [↗](#)



View Crossmark data [↗](#)



# A green and efficient route for P – S – C bond construction using copper ferrite nanoparticles as catalyst: a TD-DFT study

Firouz Matloubi Moghaddam, Maryam Daneshfar, and Reza Azaryan

Department of Chemistry, Sharif University of Technology, Tehran, Iran

## ABSTRACT

Magnetic nanoparticles of  $\text{CuFe}_2\text{O}_4$  were applied as catalyst system for one-pot thiophosphate synthesis via the reaction of aryl sulfonyl chlorides with *H*-phosphonates under conventional heating conditions. This is an extremely efficient and green method for thiophosphate synthesis under base- and solvent-free conditions. Various thiophosphates were obtained in good to excellent yields under the optimized reaction conditions in a short time. The catalyst can be easily recycled from the reaction by an external magnetic field and reused for the next run. In this study, TD-DFT B3LYP/6-31 + G(d) calculations are in good accord with the experimental results. A comparison between experimental and theoretical UV-vis absorption spectra of the thiophosphate **3k** has been carried out; and a small hypsochromic shift (only  $\sim 2\text{ nm}$ ) was displayed at maximum absorption. The aim of this work is to investigate the best method and basis set for thiophosphate compounds; therefore, predictions for these compounds can be performed in theoretical studies.

## ARTICLE HISTORY

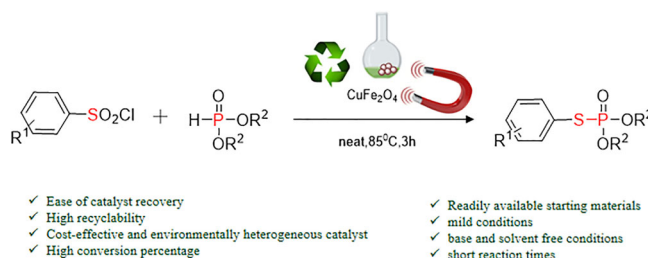
Received 15 June 2020

Accepted 3 October 2020

## KEYWORDS

Thiophosphate;  $\text{CuFe}_2\text{O}_4$ ; sulfonyl chlorides; heterogeneous catalyst; DFT; UV-visible spectroscopy

## GRAPHICAL ABSTRACT



## Introduction

Thiophosphate derivatives have attracted much attention in recent years due to their extensive pharmaceutical and agricultural applications.<sup>[1–3]</sup> They are an important class of molecules in organic synthesis because of their biological and physical properties.<sup>[4–8]</sup> A number of well-known medicines and insecticides are based on these thiophosphate derivatives. Some examples of medicines are Echthiophate (used in treatment of glaucoma) and Amifostine (used in cancer chemotherapy). Thiophosphate applications in organic synthesis are also well recognized. However, efficient and precise preparations of these thiophosphate derivatives are rather unexplored.<sup>[9–12]</sup> Traditional procedures to synthesize thiophosphate involved the reaction of trialkyl phosphites with sulfonyl chlorides by chlorinating the mercaptan or disulfide with sulfonyl chloride.<sup>[13]</sup>

Among different methods for construction of P – S – C bond,<sup>[14–16]</sup> metals can be used for coupling reactions of sulfonyl chlorides with  $\text{P}(\text{O})\text{--H}$ .<sup>[8,17–20]</sup>

In 2014, Wu's group reported the copper-catalyzed reductive cross-coupling reaction of aryl sulfonyl chlorides with *H*-phosphonates.<sup>[8]</sup> Recently, Zhang's group reported thiophosphate synthesis using aryl sulfonyl chlorides and dialkyl phosphonate in the presence of copper and L-proline as the ligand.<sup>[20]</sup>

Although many efforts have been made to facilitate the synthesis of thiophosphates, some problems exist with these procedures such as: needing fresh prepared raw materials,<sup>[13,21]</sup> using bases,<sup>[18]</sup> foul-smelling starting materials<sup>[22,23]</sup> or other additives.<sup>[20,23]</sup> Thus, the development of simple and environmental friendly synthesis methods remains unexplored.

In recent years, the green synthesis of metal oxides nanoparticles has gained extensive attention because of its feasibility and eco-friendly.<sup>[24]</sup> In green synthesis of nanoparticles, the destructive effects in applying hazardous and toxic materials are reduced which is commonly utilized in both laboratory and industry. Benefits of using catalysts in reactions are their effect on activation energy and reaction time, higher yield and lower production of by-products.<sup>[25–29]</sup>

**Table 1.** Optimization of the reaction conditions<sup>a</sup>.

Entry	Catalyst	Solvent	T (°C)	Yield <sup>b</sup> (%)
1.	–	CH <sub>3</sub> CN	85	25
2.	CoCuFe <sub>2</sub> O <sub>4</sub>	CH <sub>3</sub> CN	85	70
3.	NiFe <sub>2</sub> O <sub>4</sub>	CH <sub>3</sub> CN	85	35
4.	CuFe <sub>2</sub> O <sub>4</sub>	CH <sub>3</sub> CN	85	92
5.	CuFe <sub>2</sub> O <sub>4</sub>	1,4-dioxane	85	45
6.	CuFe <sub>2</sub> O <sub>4</sub>	THF	66	90
7.	CuFe <sub>2</sub> O <sub>4</sub>	Toluene	85	51
8.	CuFe <sub>2</sub> O <sub>4</sub>	DMF	85	NR
9.	CuFe <sub>2</sub> O <sub>4</sub>	DMSO	85	NR
10.	CuFe <sub>2</sub> O <sub>4</sub>	DCE	85	85
11.	CuFe <sub>2</sub> O <sub>4</sub>	CHCl <sub>3</sub>	60	88
12.	CuFe <sub>2</sub> O <sub>4</sub>	H <sub>2</sub> O	85	NR
13.	CuFe <sub>2</sub> O <sub>4</sub>	EtOH	85	NR
14.	CuFe <sub>2</sub> O <sub>4</sub>	EtOAc	77	90
15.	CuFe <sub>2</sub> O <sub>4</sub>	CH <sub>3</sub> CN	r.t	NR
16.	CuFe <sub>2</sub> O <sub>4</sub>	CH <sub>3</sub> CN	50	72
17.	CuFe <sub>2</sub> O <sub>4</sub> <sup>c</sup>	CH <sub>3</sub> CN	85	90
18	CuFe <sub>2</sub> O <sub>4</sub>	–	85	95

<sup>a</sup>Reaction conditions: **1a** (0.5 mmol), **2a** (2.0 mmol), catalyst (10 mol%), solvent (1 mL), 3 h.

<sup>b</sup>Isolated yield. <sup>c</sup>catalyst (20 mol%). NR = no reaction.

Herein, we wish to disclose a considerably improved method to synthesize various thiophosphates via copper ferrite catalyzed reductive cross-coupling reactions of commercially available aryl sulfonyl chlorides with dialkyl phosphonates under base and solvent free conditions. So, applying an inexpensive, heterogeneous and recyclable catalyst could be worthwhile.

## Results and discussion

Copper ferrite nanoparticles were prepared using co-precipitation method (Scheme S1 Supplemental Materials).<sup>[30,31]</sup> The synthesized nanoparticles were analyzed using various physicochemical techniques including XRD, FT-IR, VSM, FE SEM, and TEM in order to characterize the catalyst structure.

The peaks that appeared at 540 and 471 cm<sup>−1</sup> are attributed to the vibration of Cu–O and Fe–O bonds, respectively. In addition, the broad band at 3443 cm<sup>−1</sup> can be assigned to the OH groups on the surface of catalyst (Figure S1 Supplemental Materials).

The X-ray powder diffraction analysis of the copper ferrite nanoparticles is shown in Figure S2. Comparison of the all peaks of CuFe<sub>2</sub>O<sub>4</sub> nanoparticles with the standard XRD patterns (JCPDS file No: 10-325) confirms the cubic spinel structure of the catalysts. The sizes of the CuFe<sub>2</sub>O<sub>4</sub> nanoparticles are determined 48 nm from the broadening of the peak at 2θ = 35.75 using the Scherrer equation.

The magnetization curve of catalyst shows small coercivities which confirm the superparamagnetic nature of CuFe<sub>2</sub>O<sub>4</sub> nanoparticles (Figure S3).

On the other hand, morphology and structure of CuFe<sub>2</sub>O<sub>4</sub> nanoparticles were investigated by TEM analysis. CuFe<sub>2</sub>O<sub>4</sub> nanoparticles with an average size of 50 nm are mostly spherical as shown in Figure S4.

**Table 2.** Synthesis of thiophosphates from sulfonyl chlorides and H-phosphonates<sup>a</sup>.

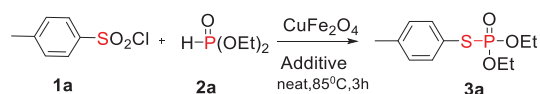
1	2	3	
			<b>3a</b> (95%)
			<b>3b</b> (83%)
			<b>3c</b> (92%)
			<b>3d</b> (80%)
			<b>3e</b> (89%)
			<b>3f</b> (78%)
			<b>3g</b> (80%)
			<b>3h</b> (68%)
			<b>3i</b> (65%)
			<b>3j</b> (53%)
			<b>3k</b> (93%)
			<b>3l</b> (81%)

<sup>a</sup>Reaction conditions: **1a** (0.5 mmol), **2a** (2.0 mmol), catalyst (10 mol%), 3 h. Isolated yield in parentheses.

After confirming the formation of copper ferrite, we started our investigation by introducing tosyl chloride (**1a**) with diethyl phosphonate (**2a**) as model substrates to optimize the reaction conditions. Effect of different parameters such as catalyst sources, solvents and reaction temperature was surveyed. The results are shown in Table 1. The absence of metal led to disappointing result (Table 1, entry 1). Next, the catalytic efficiency of different ferrite nanoparticles were studied and found that CuFe<sub>2</sub>O<sub>4</sub> nanoparticles were the best choice for this reaction (entries 2–4). Indeed, copper has a critical role in this reductive cross-coupling reaction. A variety of polar and nonpolar solvents such as CHCl<sub>3</sub>, dioxane, toluene, and DMSO were applied (entries 5–14). Among them acetonitrile was the optimal choice and selected for the rest of optimization condition.

At last, the effect of temperature on the reaction was investigated (entries 15–16). We found that 85 °C was the optimal temperature with high reaction conversion (entry 3). Unfortunately, the P–S–C bond transformation was not accelerated at room temperature. On the other hand, increasing the amount of the catalyst from 10% to 20% slightly improved the yield (entry 17). The yield improved to 95% in the absence of solvent (entry 18). The ratio of **1a** and **2a** was chosen 1: 4 because byproducts such as disulfides and thiosulfonates were not generated by using excess amount of diethyl phosphonate. Also, diethyl phosphonate as a main byproduct was isolated, which consumed a portion of the reagent. So, the ratio of substrates played an important role in this reaction.

After determining the optimized conditions, the scope of the substrates was examined. It was pleasing to find that dimethyl phosphonate and diethyl phosphonate could couple with different sulfonyl chlorides in desired yields. Various



Additives	3a, Yield(%)
None	95
BHT (2.0 equiv)	86
TEMPO (2.0 equiv)	81

**Scheme 1.** Radical inhibition experiments.

aryl sulfonyl chlorides bearing both electron-donating and electron-withdrawing groups can be tested under the defined conditions. The results are shown in Table 2. Aryl sulfonyl chloride bearing weak electron-donating and neutral groups resulted in good yields (Table 2, 3a-3d) while electron-withdrawing groups led to lower yields of thiophosphates (Table 2, 3i-3j). Compared with the previous report, the yield of compound 3i was increased to 65% when the reaction proceeded using  $\text{CuFe}_2\text{O}_4$ .<sup>[14]</sup>

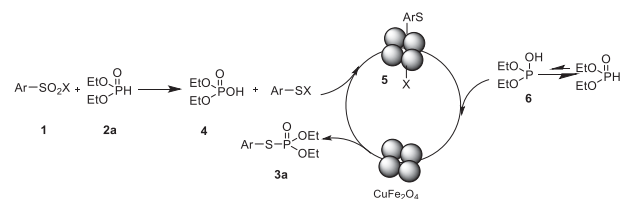
In addition, the halogen groups such as 4-chloro and 4-bromo benzenesulfonyl chlorides remained intact in the products, and they can undergo for further useful transformation (Table 2, 3e-3h). We also applied these reaction conditions for 1-naphthalenesulfonylchloride as a substrate to investigate the applicability of the procedure. The desired corresponding products 3k and 3l were obtained in 93% and 81% yields, respectively.

To gain the mechanism insights, the reaction of tosyl chloride (1a) with diethyl phosphonate (2a) was performed in the presence of 2,2,6,6-tetramethylpiperidine-1-oxyl (TEMPO) and 2,6-di-tert-butyl-4-methylphenol (BHT) as radical scavengers. The results indicated that the reaction does not proceed through a radical pathway because no significant decrease of the product was observed (Scheme 1).

On the basis of our experiment results and previous reports, a plausible mechanism of the reaction between aryl sulfonyl halide and diethyl phosphonate was proposed (Scheme 2). First, diethyl phosphonate deoxygenate sulfonyl halide to form sulfinyl halide and diethyl phosphate 4 (confirmed by NMR in this work). Then, the generated sulfinyl halide reacts with copper ferrite to produce intermediate 5 which adds to tautomerized form of diethyl phosphonate 6. The desired product is released and copper ferrite was regenerated to fulfill the catalytic cycle. In support of this mechanistic speculation, disulfides and thiosulfonates were not observed as intermediates during the reaction followed by GC.

The reusability of the catalyst was studied. First, the catalyst was separated from the reaction mixture by a magnetic rod, washed with methanol and water. Then, dried on air for the next run. According to the results shown in Figure S5 no appreciable loss of activity was observed up to 5 cycles.

To evaluate the efficiency of the present protocol, examples of the same reactions performed with different catalysts



**Scheme 2.** Proposed mechanism.

**Table 3.** Comparison of the catalytic efficiency of  $\text{CuFe}_2\text{O}_4$  with other catalysts for the synthesis of thiophosphates.

Entry	Catalyst	Solvent	Temperature (OC)	Time (h)	Additive	References
1	$\text{Cu}(\text{OAc})_2$	$\text{CH}_3\text{CN}$	140	24	–	[8]
2	$\text{CuCl}_2 \cdot 2\text{H}_2\text{O}$	THF	80	12	L- Proline	[20]
3	Pd/dppf	Toluene	100	20	styrene	[11]
4	$\text{Ni}(\text{OAc})_2 / \text{Y}(\text{OTf})_3$	DMF	70	24	–	[32]
5	$\text{CuFe}_2\text{O}_4$	–	85	3	–	This Work

are listed in Table 3. For example, in Entry 1 reaction run under harsh condition such as high temperature and long reaction time. In Entry 2 the reaction time and temperature are reduced but it still needs additive and solvent. In Entries 3-4 expensive catalysts are employed and the starting materials are foul-smelling. It is obvious that in this strategy the reaction time and temperature have been decreased to 3 h and 85°C (Entry 5). It is a green method for thiophosphate synthesis because in these conditions we do not need any base, ligand, additive or solvent. Starting materials in this procedure are not foul-smelling and the catalyst is cheap, recyclable and reusable with an external magnetic field. The yields indicate that the  $\text{CuFe}_2\text{O}_4$  catalyst nanoparticles have high activity the same as the homogeneous catalysts which have been reported in literature.<sup>[8,11,20,32]</sup>

The FE SEM images confirmed that morphology and dispersity of the catalyst are not changed during these runs (Figure S6). Therefore, no significant loss in catalyst activity, size or morphology was observed.

Moreover, UV-vis properties of the thiophosphate compounds have not been investigated up to now. An important aim of this work is to find the best method and basis set to be compatible with experimental data. Therefore, the method and basis set can be used to gain further information in theoretical studies and predict properties of thiophosphates. Figure S7, shows optimized structure of compound 3k.

In order to reproduce the UV-visible spectra of 3k, calculations performed by employing TD-DFT methods at the B3LYP/6-31 + G(d) level of theory. Excitation energies were computed for the first 25 excited states and the polarizable continuum model (PCM) method was employed in Ethanol as solvent.

In Figure S8, the experimental and calculated spectra for the compound 3k are investigated. It shows that both experimental and calculated spectra of the investigated compound are in good agreement. The experimental spectrum displays maximum absorption at 223 nm. According to TD-DFT calculations, there is absorption band at 225

( $f=0.8378$ ). The absorption band at 225 nm had a small hypsochromic shift ( $\sim 2$  nm) compared with the experimental band at 223 nm.

The distribution of the HOMO orbital was located on the sulfur atom (S); meanwhile the LUMO orbital (see Figure S9) was uniformly distributed along the two rings with little distribution on the phosphorus atom (P).

Difference between transition energy levels is called gap energy.<sup>[33]</sup> The HOMO – LUMO energy gap of **3k** is about  $-1.86$  eV represented in Figures S9.

It is necessary to mention that a predicted electronic transition at 225 nm is not mainly HOMO LUMO.

There are other important contributions of the electronic transitions like HOMO LUMO + 1 or HOMO –1 LUMO.

For electrophilic and nucleophilic attack reactive sites of the **3k** can be predicted by employing the MEP at the B3LYP/6-31 + G(d) of the optimized geometry. In a MEP map, the positive regions (blue color) correlated to nucleophilic attack and the negative regions (red or yellow color) are correlated to electrophilic attack, as displayed in Figure S10.

In compound **3k** the color code of the map is in the range between  $-0.118$  a.u. (deepest red) and  $0.118$  a.u. (deepest blue). As can be seen from the Figure S10, this molecule has a probable site for electrophilic attack. Based on the results, the MEP map shows that the negative potential sites are mainly over  $O_{13}$  ( $P_{12}=O_{13}$  double bond) which is an electronegative atom. Green areas cover predominant parts of the molecule where electrostatic potentials are nearly zero and observed mostly on phenyl rings or methyl groups.

## Conclusions

In summary, we have described copper ferrite nanoparticles as a very efficient heterogeneous catalytic system in coupling of P(O)–H with sulfonyl chlorides under relatively mild conditions.

The proposed conditions applied here for synthesis of thiophosphates compared to previous reports using other homogeneous catalytic systems lead to a green procedure in a short time. In this procedure solvent, base, ligand and additive have been omitted. Time and temperature decreased significantly and provided a more attractive pathway for the synthesis of biological and agricultural useful thiophosphate compounds under green conditions. In addition, inexpensive, recyclable and reusable ferromagnetic copper ferrite nanoparticles as catalyst make this method practical and highly attractive. It is obvious that none of starting materials are foul-smelling and evaluate the efficiency of this procedure.

Furthermore, application of B3LYP density functional along with the 6-31 + G(d) basis set for UV-vis spectra calculations provides minimum absolute deviation from the experimental values (only  $\sim 2$  nm). There is a synergistic relationship between the experimental and theoretical findings. Thus, the method and basis set can be used to gain further information in theoretical studies and predict properties of these thiophosphate compounds due to the high accuracy in experimental and theoretical results.

## Experimental

### Materials and characterization methods

$^1\text{H}$  NMR were recorded on a Bruker AVANCE DRX 500 MHz NMR spectrometer with  $\text{CDCl}_3$  as solvent and tetramethylsilane (TMS) as internal standard or  $\text{H}_3\text{PO}_4$  as internal standard for  $^{31}\text{P}$  NMR. The UV–Vis spectrum were measured using a Perkin Elmer Lambda 25 spectrophotometer. The IR spectrum were collected in the solid state using an ABB Bomem MB-100 FT-IR spectrophotometer in the range of  $4000$  to  $400\text{ cm}^{-1}$ . The instrument used for mass analyses was an Agilent (Agilent Technologies, Palo Alto, CA, USA) using ESI (electrospray ionization) and equipped with a 5973 quadrupole mass spectrometer. XRD analysis of the catalyst were carried out using Siemens D5000 X-ray diffractometer with  $\text{Cu-K}\alpha$  radiation. The morphology of the catalyst was characterized by FE SEM (MIRA3 TESCAN-RMRC) and TEM (TECNAI F20). To determine magnetic properties of the catalyst, vibrating sample magnetometer at Kashan University of Iran was carried out. The Supplemental Materials contains sample  $^1\text{H}$ ,  $^{13}\text{C}$  and  $^{31}\text{P}$  NMR spectra of the products (Figures S11 – S39).

### General procedure for synthesis of thiophosphates from sulfonyl chlorides and H-phosphonates

In a glass tube, sulfonyl chlorides ( $0.5$  mmol), H-phosphonates ( $2.0$  mmol) and  $\text{CuFe}_2\text{O}_4$  ( $10$  mol%) were added and heated at  $85^\circ\text{C}$  for  $3$  h. The completion of the reaction was monitored by TLC.  $\text{CuFe}_2\text{O}_4$  nanoparticles were collected with a magnet and the mixture was diluted with  $10$  mL of water. Then, product was extracted with EtOAc ( $4 \times 10$  mL).

The organic layer was washed with brine, dried ( $\text{Na}_2\text{SO}_4$ ) and evaporated under vacuum. Finally, the crude product was purified by column chromatography on silica gel and eluted with petroleum ether/ethyl acetate ( $1:1$ ). Thiophosphates product appear as a yellow oil.

### Supporting information summary

The structures of all compounds were characterized by spectroscopic methods (FT-IR,  $^1\text{H}$  NMR,  $^{31}\text{P}$  NMR,  $^{13}\text{C}$  NMR Mass). The absorption behaviors of selected compounds were investigated with UV-Vis spectroscopy in ethanol. Computation details and spectra of products are given in the supporting information for this article.

### Funding

We gratefully acknowledge the funding support received for this project from the Sharif University of Technology (SUT), Islamic Republic of Iran.

## References

- [1] He, W.; Wang, Z.; Li, X.; Yu, Q.; Wang, Z. Direct Synthesis of Thiophosphates by Reaction of Diphenylphosphine Oxide with Sulfonyl Chlorides. *Tetrahedron* **2016**, *72*, 7594–7598. DOI: 10.1016/j.tet.2016.10.012.



- [2] Xie, R.; Zhao, Q.; Zhang, T.; Fang, J.; Mei, X.; Ning, J.; Tang, Y. Design, Synthesis and Biological Evaluation of Organophosphorous-Homodimers as Dual Binding Site Acetylcholinesterase Inhibitors. *Bio. Med. Chem.* **2013**, *21*, 278–282. DOI: [10.1016/j.bmc.2012.10.030](https://doi.org/10.1016/j.bmc.2012.10.030).
- [3] Noro, M.; Fujita, S.; Wada, T. Stereoselective Synthesis of P-Modified  $\alpha$ -Glycosyl Phosphates by the Oxazaphospholidine Approach. *Org. Lett.* **2013**, *15*, 5948–5951. DOI: [10.1021/ol402785h](https://doi.org/10.1021/ol402785h).
- [4] Guga, P.; Boczkowska, M.; Janicka, M.; Maciaszek, A.; Nawrot, B.; Antoszczyk, S.; Stec, W. J. Enhanced P-Stereodependent Stability of Complexes Formed by Phosphorothioate Oligonucleotides Due to Involvement of Sulfur as Strong Hydrogen Bond Acceptor. *Pure Appl. Chem.* **2006**, *78*, 993–1002. DOI: [10.1351/pac200678050993](https://doi.org/10.1351/pac200678050993).
- [5] Lauer, A. M.; Mahmud, F.; Wu, J. Cu(I)-catalyzed,  $\alpha$ -selective, allylic alkylation reactions between phosphorothioate esters and organomagnesium reagents. *J. Am. Chem. Soc.* **2011**, *133*, 9119–9123. DOI: [10.1021/ja202954b](https://doi.org/10.1021/ja202954b).
- [6] Lauer, A. M.; Wu, J. Palladium-Catalyzed Allylic Fluorination of Cinnamyl Phosphorothioate Esters. *Org. Lett.* **2012**, *14*, 5138–5141. DOI: [10.1021/ol302263m](https://doi.org/10.1021/ol302263m).
- [7] Li, N.-S.; Frederiksen, J. K.; Piccirilli, J. A. Synthesis, Properties, and Applications of Oligonucleotides Containing an RNA Dinucleotide Phosphorothiolate Linkage. *Acc. Chem. Res.* **2011**, *44*, 1257–1269. DOI: [10.1021/ar200131t](https://doi.org/10.1021/ar200131t).
- [8] Bai, J.; Cui, X.; Wang, H.; Wu, Y. Copper-Catalyzed Reductive Coupling of Aryl Sulfonyl Chlorides with H-Phosphonates Leading to S-Aryl Phosphorothioates. *Chem. Commun.* **2014**, *50*, 8860–8863. DOI: [10.1039/c4cc02693d](https://doi.org/10.1039/c4cc02693d).
- [9] Huang, H.; Ash, J.; Kang, J. Y. Base-Controlled Fe(Pc)-Catalyzed Aerobic Oxidation of Thiols for the Synthesis of S-S and S-P(O) bonds. *Org. Biomol. Chem.* **2018**, *16*, 4236–4242. DOI: [10.1039/c8ob00908b](https://doi.org/10.1039/c8ob00908b).
- [10] Quin, L. D. *A Guide to Organophosphorus Chemistry*; John Wiley & Sons: New York, **2000**.
- [11] Zhu, Y.; Chen, T.; Li, S.; Shimada, S.; Han, L. B. Efficient Pd-Catalyzed Dehydrogenative Coupling of P(O)H with RSH: A Precise Construction of P(O)-S Bonds. *J. Am. Chem. Soc.* **2016**, *138*, 5825–5828. DOI: [10.1021/jacs.6b03112](https://doi.org/10.1021/jacs.6b03112).
- [12] Kumar, T. S.; Yang, T.; Mishra, S.; Cronin, C.; Chakraborty, S.; Shen, J.-B.; Liang, B. T.; Jacobson, K. A. 5'-Phosphate and 5'-phosphonate ester derivatives of (N)-methanocarba adenosine with in vivo cardioprotective activity. *J. Med. Chem.* **2013**, *56*, 902–914. DOI: [10.1021/jm301372c](https://doi.org/10.1021/jm301372c).
- [13] Morrison, D. The Reaction of Sulfonyl Chlorides with Trialkyl Phosphites. *J. Am. Chem. Soc.* **1955**, *77*, 181–182. DOI: [10.1021/ja01606a062](https://doi.org/10.1021/ja01606a062).
- [14] Wang, J.; Huang, X.; Ni, Z.; Wang, S.; Pan, Y.; Wu, J. Peroxide Promoted Metal-Free Thiolation of Phosphites by Thiophenols/Disulfides. *Tetrahedron* **2015**, *71*, 7853–7859. DOI: [10.1016/j.tet.2015.08.025](https://doi.org/10.1016/j.tet.2015.08.025).
- [15] Sun, J.-G.; Weng, W.-Z.; Li, P.; Zhang, B. Dimethyl Sulfoxide as a Mild Oxidant in S-P (O) bond Construction: simple and Metal-Free Approaches to Phosphinothioates. *Green Chem.* **2017**, *19*, 1128–1133. DOI: [10.1039/C6GC03115C](https://doi.org/10.1039/C6GC03115C).
- [16] Sun, J.-G.; Yang, H.; Li, P.; Zhang, B. Metal-Free Visible-Light-Mediated Oxidative Cross-Coupling of Thiols with P(O)H Compounds Using Air as the Oxidant. *Org. Lett.* **2016**, *18*, 5114–5117. DOI: [10.1021/acs.orglett.6b02563](https://doi.org/10.1021/acs.orglett.6b02563).
- [17] Gao, Y.-X.; Tang, G.; Cao, Y.; Zhao, Y.-F. A Novel and General Method for the Formation of S-Aryl Se-Aryl, and Te-Aryl Phosphorochalcogenoates. *Synthesis* **2009**, *2009*, 1081–1086. DOI: [10.1055/s-0028-1088012](https://doi.org/10.1055/s-0028-1088012).
- [18] Kaboudin, B.; Abedi, Y.; Kato, J.-y.; Yokomatsu, T. Copper (I) iodide Catalyzed Synthesis of Thiophosphates by Coupling of H-Phosphonates with Benzenethiols. *Synthesis* **2013**, *45*, 2323–2327. DOI: [10.1055/s-0033-1339186](https://doi.org/10.1055/s-0033-1339186).
- [19] Xu, J.; Zhang, L.; Li, X.; Gao, Y.; Tang, G.; Zhao, Y. Phosphorothiolation of Aryl Boronic Acids Using P(O)H Compounds and Elemental Sulfur. *Org. Lett.* **2016**, *18*, 1266–1269. DOI: [10.1021/acs.orglett.6b00118](https://doi.org/10.1021/acs.orglett.6b00118).
- [20] Zhang, X.; Wang, D.; An, D.; Han, B.; Song, X.; Li, L.; Zhang, G.; Wang, L. Cu(II)/Proline-Catalyzed Reductive Coupling of Sulfuryl Chloride and P(O)-H for P-S-C Bond Formation. *J. Org. Chem.* **2018**, *83*, 1532–1537. DOI: [10.1021/acs.joc.7b02608](https://doi.org/10.1021/acs.joc.7b02608).
- [21] Hoffmann, F. W.; Moore, T. R.; Kagan, B. The Reaction between Triethyl Phosphite and Alkyl and Aryl-Sulfonyl Chlorides. *J. Am. Chem. Soc.* **1956**, *78*, 6413–6414. DOI: [10.1021/ja01605a033](https://doi.org/10.1021/ja01605a033).
- [22] Arisawa, M.; Ono, T.; Yamaguchi, M. Rhodium-Catalyzed Thiophosphinylation and Phosphinylation Reactions of Disulfides and Diselenides. *Tetrahedron Lett.* **2005**, *46*, 5669–5671. DOI: [10.1016/j.tetlet.2005.06.109](https://doi.org/10.1016/j.tetlet.2005.06.109).
- [23] Bi, X.; Li, J.; Meng, F.; Wang, H.; Xiao, J. DCDMH-Promoted Synthesis of Thiophosphates by Coupling of H-Phosphonates with Thiols. *Tetrahedron* **2016**, *72*, 706–711. DOI: [10.1016/j.tet.2015.12.020](https://doi.org/10.1016/j.tet.2015.12.020).
- [24] Nguyen, N. H.; Padil, V. V. T.; Slaveykova, V. I.; Černík, M.; Ševců, A. Green Synthesis of Metal and Metal Oxide Nanoparticles and Their Effect on the Unicellular Alga *Chlamydomonas reinhardtii*. *Nanoscale Res. Lett.* **2018**, *13*, 1–13. DOI: [10.1186/s11671-018-2575-5](https://doi.org/10.1186/s11671-018-2575-5).
- [25] Parsa, F.; Ghorbanloo, M.; Masoomi, M. Y.; Morsali, A.; Junk, P. C.; Wang, J. Ultrasound-assisted synthesis and characterization of a new metal-organic framework based on azobenzene-4,4-dicarboxylic acid: Precursor for the fabrication of Co3O4 nano-particles. *Ultrasonics Sonochem* **2018**, *45*, 197–203. DOI: [10.1016/j.ultrasonch.2018.03.014](https://doi.org/10.1016/j.ultrasonch.2018.03.014).
- [26] Mohammadi, M.; Rezaei, A.; Khazaei, A.; Xuwei, S.; Huajun, Z. Correction to “Targeted Development of Sustainable Green Catalysts for Oxidation of Alcohols via Tungstate-Decorated Multifunctional Amphiphilic Carbon Quantum Dots”. *ACS Appl. Mater. Interfaces* **2019**, *11*, 43796–43796. DOI: [10.1021/acsami.9b18035](https://doi.org/10.1021/acsami.9b18035).
- [27] Zhang, N. N.; Bigdeli, F.; Miao, Q.; Hu, M. L.; Morsali, A. Ultrasonic-Assisted Synthesis, Characterization and DNA Binding Studies of Ru (II) Complexes with the Chelating N-Donor Ligand and Preparing of RuO2 Nanoparticles by the Easy Method of Calcination. *J. Organomet. Chem.* **2018**, *878*, 11–18. DOI: [10.1016/j.jorganchem.2018.09.024](https://doi.org/10.1016/j.jorganchem.2018.09.024).
- [28] Zarekarizi, F.; Beheshti, S.; Morsali, A. Solid-State Preparation of Mixed Metal-Oxides Nanostructure from Anionic Metal-Organic Framework via Cation Exchange Process. *Inorg. Chem. Commun.* **2018**, *97*, 144–148. DOI: [10.1016/j.inoche.2018.09.020](https://doi.org/10.1016/j.inoche.2018.09.020).
- [29] Safarifar, V.; Morsali, A. Facile Preparation of Nanocubes Zinc-Based Metal-Organic Framework by an Ultrasound-Assisted Synthesis Method; Precursor for the Fabrication of Zinc Oxide Octahedral Nanostructures. *Ultrasonics Sonochem* **2018**, *40*, 921–928. DOI: [10.1016/j.ultrasonch.2017.09.014](https://doi.org/10.1016/j.ultrasonch.2017.09.014).
- [30] Moghaddam, F. M.; Daneshfar, M.; Azaryan, R.; Pirat, J.-L. Copper Ferrite Nanoparticles Catalyzed Formation of  $\beta$ -Ketophosphonates via Oxyphosphorylation of Styrenes with H-Phosphonates: A DFT Study on UV-Vis Absorption Spectra. *Catal. Commun.* **2020**, *141*, 106015. DOI: [10.1016/j.catcom.2020.106015](https://doi.org/10.1016/j.catcom.2020.106015).
- [31] Moghaddam, F. M.; Pourkaveh, R.; Gholamtajari, M. Nano CoCuFe2O4-Catalyzed Coupling Reaction of Arylboronic Acid with Amines and Thiols: An Atom-Economic and Ligand-Free Route to Access Unsymmetrical Amines and Sulfides. *Appl. Organometal. Chem.* **2018**, *32*, e4568. DOI: [10.1002/aoc.4568](https://doi.org/10.1002/aoc.4568).
- [32] Xue, J. W.; Zeng, M.; Zhang, S.; Chen, Z.; Yin, G. Lewis Acid Promoted Aerobic Oxidative Coupling of Thiols with Phosphonates by Simple Nickel(II) Catalyst: Substrate Scope and Mechanistic Studies. *J. Org. Chem.* **2019**, *84*, 4179–4190. DOI: [10.1021/acs.joc.9b00194](https://doi.org/10.1021/acs.joc.9b00194).
- [33] Prasad, M.; Sri, N. U.; Veeraiah, V. A Combined Experimental and Theoretical Studies on FT-IR, FT-Raman and UV-vis spectra of 2-chloro-3-quinolinecarboxaldehyde. *Spectrochimica Acta Part A: Mol. Biomol. Spect.* **2015**, *148*, 163–174. DOI: [10.1016/j.saa.2015.03.105](https://doi.org/10.1016/j.saa.2015.03.105).